**Int. J. Contemp. Math. Sciences, Vol. 6, 2011, no. 22, 1051 - 1070**

# Vibration Reduction and Stability of Non-Linear System Subjected to External and Parametric Excitation Forces under a Non-Linear Absorber

**M. Sayed [1*], Y. S. Hamed [1*] and Y. A. Amer [**]**

[1] Department of Mathematics and Statistics, Faculty of Science, Taif University
El-Taif, El-Haweiah, P.O. Box 888, Zip Code 21974, Kingdom of Saudi Arabia
eng_yaser_salah@yahoo.com

* Faculty of Electronic Engineering, Menoufia University, Menouf 32952, Egypt

** Department of Mathematics, Faculty of Science, Zagazig University
Zagazig, Egypt

**Abstract**

Vibrations are usually undesired phenomena as they may cause discomfort, disturbance, damage, and sometimes destruction of machines and structures. It must be reduced or controlled or eliminated. One of the most common methods of vibration control is the dynamic absorber. In this paper, the non-linear dynamics of a two-degree-of freedom vibration system including quadratic and cubic non-linearities subjected to external and parametric excitation forces is investigated. The system consists of the main system and the absorber which represents many applications in machine tools, ultrasonic cutting process, etc. The vibration of the main system can be controlled applying non-linear absorber (passive control). The stability of the system is investigated using both frequency response curves and phase-plane trajectories. Multiple time scales perturbation method is applied to differential equations describing the system to obtain the analytical solution. All possible resonance cases are extracted. The effects of different parameters of the system are studied numerically. There exist multi-valued solutions which increase or decrease by the variation of some parameters. The solution loses stability on increasing negative value of $\alpha_2$. The Numerical simulations show the system exhibits periodic motions and chaotic motions. A comparison is made with the available published work.

**Keywords**: Non-linear vibration; response; stability; resonance; jump phenomenon

## 1. Introduction

The dynamic response of mechanical and civil structures subject to high-amplitude vibration is often dangerous and undesirable. Sometimes controlled vibration is desirable as in ultrasonic machining (USM), as the machining technique is dependent on tool and abrasive particles vibration. It is required to reduce the vibration in the machine head and have reasonable amplitude for the tools. This can be done via dynamic absorber. It has the advantages of low cost and simple operation at one modal frequency. In the domain of many mechanical vibration systems the coupled non-linear vibration of such systems can be reduced to non-linear second order differential equations which are solved analytically and numerically. Queini and Nayfeh [1] proposed a non-linear active control law to suppress the vibrations of the first mode of a cantilever beam when subjected to a principal parametric excitation. The method of multiple scales is applied throughout. The analysis revealed that cubic velocity feedback reduced the amplitude of the response. Asfar [2] took material non-linearity into consideration in the analysis of the performance of an elastomeric damper with a spring hardening cubic effects near primary resonance condition applying multiple time scale method. Eissa [3] reported that when using a dynamic absorber, its damping coefficient should be kept minimal for better system performance. Eissa [4] has shown that for controlling the vibration of a system subjected to harmonic excitations, the fundamental or the first harmonic absorber is the most effective one. Eissa and El-Ganaini [5, 6] studied the control of both vibration and dynamics chaos of mechanical system having quadratic and cubic non-linearities, subjected to harmonic excitation using multi-absorbers. Kamel and Amer [7] studied the behavior of one-degree-of-freedom system with different quadratic damping and cubic stiffness non-linearities simulating the axial vibration of a cantilever beam under multi-parametric excitation forces. Song et al. [8] investigated the vibration response of the spring mass damper system with a parametrically excited pendulum hinged to the mass using the harmonic balance method. The stability analysis showed that the area of unstable motion of the system obtained from the third order approximation.

Soom [9] and Jordanov [10] studied the optimal parameter design of linear and non-linear dynamic vibration absorbers for damped primary systems. They examined optimization criteria other than the traditional one and obtained small improvements in steady state response by using non-linear springs. However, the presence of the non-linearities introduces dangerous instability, which in some cases may result in amplification rather than reduction of the vibration amplitudes [11, 12]. Natsiavas [13] applied the method of averaging to investigate the steady state oscillations and stability of non-linear dynamic vibration absorbers. He pointed out that proper selection of the system parameters would result

insubstantial improvements of non-linear absorbers and avoid dangerous effects that are likely to occur due to the presence of the non-linearities. Zhu et al. [14] studied the non-linear dynamics of a two-degree-of freedom vibrating system having both non-linear damping and non-linear spring using the averaging method. Results showed that the vibration amplitude can be reduced by properly selecting the values of non-linear damper, non-linear spring stiffness and the range of exciting frequency.

Lim et al. [15] investigated the behavior of the (USM) hypothesized theoretical model which described by the coupling of two non-linear oscillators. The method of multiple scales has been used to solve the equations to first order perturbation. The theoretical results showed that controlled variations in the softening stiffness can have a significant effect on the overall non-linear response of the system, by making the overall effect hardening, softening, or approximately linear. Experimentally, it has also been demonstrated that coupling of ultrasonic components with different non-linear characteristics can strongly influence the performance of the system. Eissa and Amer [16] simulated the vibration of a second order system to the first mode of a cantilever beam subjected to both external and parametric excitation at primary and sub-harmonic resonance. They analyzed the system using the method of multiple scales. They reported that the vibration of the system can be controlled by adding a feedback cubic non-linear term. They reported also that there is a threshold value for the linear damping coefficient which can be applied to control the system vibration. Nayfeh [17] compared application of the method of multiple scales with reconstitution and the generalized method of averaging for determining higher-order approximations of three single-degree-of-freedom systems and a two-degree-of-freedom system. He showed that the second-order frequency-response equation possesses spurious solutions for the case of softening nonlinearity. El-Bassiouny [18] investigated the effects of quadratic and cubic non-linearities in elastomeric material dampers on torsional vibration control. The multiple time scale is used to solve the stability equations at primary resonance. He showed that the elastomeric damper reduced the vibration of the crankshaft effectively. Eissa et al. [19, 20] presented the tuned absorber in both transversely and longitudinal directions of a simple pendulum which designed to control one frequency at primary resonance. The multiple time scale perturbation technique is applied throughout. They demonstrated the effectiveness of the absorber for passive control. They reported that the vibration of the system can be controlled actively via negative velocity feedback, which can be used to reduce the amplitude of the system. Amer [21] investigated the coupling of two non-linear oscillators of main system and absorber representing ultrasonic cutting process subjected to parametric excitation forces. A threshold value of main system linear damping has been obtained, where vibration can be reduced dramatically. This threshold value can be used effectively for passive vibration control, if it is economical. The multiple time scale perturbation technique is applied throughout. A threshold value of linear damping has been obtained, where the system vibration can be reduced dramatically.

Hamed et al. [23-25] studied USM model subject to multi-external or both multi-external and multi-parametric and both multi-external and tuned excitation forces. The model consists of multi-degree-of-freedom system consisting of the tool holder and absorbers (tools) simulating ultrasonic machining process. The advantages of using multi-tools are to machine different materials and different shapes at the same time. This leads to time saving and higher machining efficiency.

## 2. Passive Control

Using a non-linear tuned mass absorber connected to the main system, a model of a two degree-of-freedom oscillator under consideration is shown in Fig.1, from the principles of the mechanics, the derived equations of motion can be written in the forms:

$$\ddot{x}_1 + \omega_1^2 x_1 + \varepsilon\alpha_1 x_1^2 + \varepsilon\alpha_2 x_1^3 + \varepsilon\zeta_1 \dot{x}_1 + \varepsilon\zeta_2 \dot{x}_1 x_1^2 + \varepsilon\zeta_3(\dot{x}_1 - \dot{x}_2) - \varepsilon\alpha_3 x_2 + \varepsilon\alpha_4(x_1 - x_2)^2 + \varepsilon\alpha_5(x_1 - x_2)^3 = \varepsilon F_1 \cos\Omega_1 t + \varepsilon x_1 F_2 \cos\Omega_2 t \quad (1)$$

$$\ddot{x}_2 + \omega_2^2(x_2 - x_1) + \varepsilon\beta_1(x_2 - x_1)^2 + \varepsilon\beta_2(x_2 - x_1)^3 + \varepsilon\zeta_4(\dot{x}_2 - \dot{x}_1) = 0 \quad (2)$$

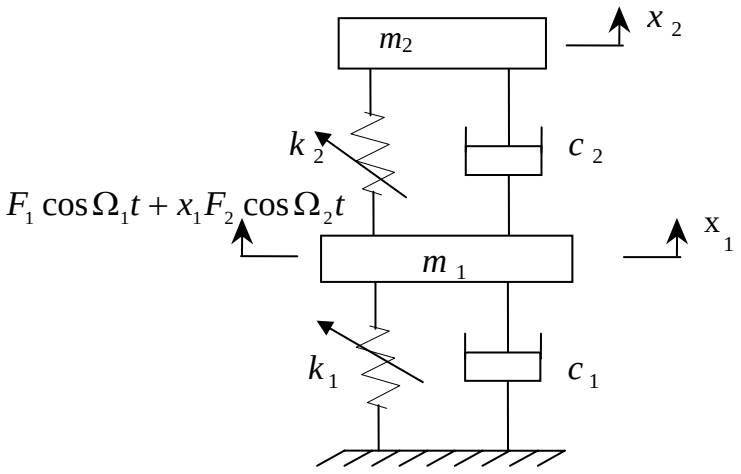


Fig.1. Schematic diagram of the model with absorber.

where

$$\omega_1^2 = \frac{k_{11} + k_{21}}{m_1}, \alpha_1 = \frac{k_{12}}{m_1}, \alpha_2 = \frac{k_{13}}{m_1}, \zeta_1 = \frac{c_1}{m_1}, \zeta_2 = \frac{c_2}{m_1}, \zeta_3 = \frac{c_3}{m_1}, \alpha_3 = \frac{k_{21}}{m_1}, ,$$

$$\alpha_4 = \frac{k_{22}}{m_1}, \alpha_5 = \frac{k_{23}}{m_1}, \quad F_j = \frac{f_j}{m_1}, \omega_2^2 = \frac{k_{21}}{m_2}, \zeta_4 = \frac{c_3}{m_2}, \beta_1 = \frac{k_{22}}{m_2}, \beta_2 = \frac{k_{23}}{m_2}$$

$c_1$, $c_2$ are the damping coefficients of the main system and absorber, $c_3$ the coupling damping coefficient, $m_1$, $m_2$ the mass of the main system and absorber,

$\Omega_j$ ( $j$=1, 2 ) forcing frequencies, $\omega_1$, $\omega_2$ natural frequencies, $k_{11}$, $k_{21}$ linear stiffness, $x_1, x_2$ displacement of the main system and absorber, $\dot{x}_j$, $\ddot{x}_j$ derivatives of $x$ w. r. t time, $\varepsilon$ small perturbation parameter, $f_j$ the forcing amplitudes, $\alpha_i, \beta_j$ non-linear parameters ($i$ =1,…,5), $\zeta_S$ damping coefficient ($s$ =1, …, 4).

## 3. Method of Analysis

A first-order uniform solution of equations (1)-(2) is sought using the method of multiple scales [22] in the form:

$$x_1(t;\varepsilon) = x_{10}(T_0,T_1) + \varepsilon x_{11}(T_0,T_1) + \ldots \tag{3}$$

$$x_2(t;\varepsilon) = x_{20}(T_0,T_1) + \varepsilon x_{21}(T_0,T_1) + \ldots \tag{4}$$

where $T_o$= $t$ is fast time scale, which is associated with changes occurring at the frequencies $\omega_j$ and $\Omega_j$ and $T_1$= $\varepsilon t$ is the slow time scale, which is associated with modulations in the amplitudes and phases resulting from the non-linearities and parametric resonance. In term of $T_o$ and $T_1$ the time derivatives became

$$\frac{d}{dt} = D_0 + \varepsilon D_1 + \ldots \quad , \quad \frac{d^2}{dt^2} = D_0^2 + 2\varepsilon D_0 D_1 + \ldots \tag{5}$$

Where $D_n$ differential operators; $D_n = \partial / \partial T_n$ $(n = 0,1)$. Substituting equations (3) and (4) into equations (1)-(2) and equating the coefficients of same power of $\varepsilon$ in both sides, we obtain:

Order $\varepsilon^0$ : $(D_0^2 + \omega_1^2)x_{10} = 0$ (6)

$$(D_0^2 + \omega_2^2)x_{20} = \omega_2^2 x_{10} \tag{7}$$

Order $\varepsilon$ :

$$\begin{aligned}(D_0^2 + \omega_1^2)x_{11} = {} & F_1\cos(\Omega_1 T_0) + x_{10}F_2\cos(\Omega_2 T_0) - 2D_0D_1x_{10} - \alpha_1 x_{10}^2 - \alpha_2 x_{10}^3 \\ & -\zeta_1 D_0 x_{10} - \zeta_2 (D_0 x_{10})x_{10}^2 - \zeta_3 (D_0 x_{10} - D_0 x_{20}) + \alpha_3 x_{20} - \alpha_4 (x_{10}^2 \\ & -2x_{10}x_{20} + x_{20}^2) - \alpha_5 (x_{10}^3 - 3x_{10}^2 x_{20} + 3x_{10}x_{20}^2 - x_{20}^3)\end{aligned} \tag{8}$$

$$\begin{aligned}(D_0^2 + \omega_2^2)x_{21} = {} & -2D_0D_1x_{20} + \omega_2^2 x_{11} - \beta_1 (x_{20}^2 - 2x_{20}x_{10} + x_{10}^2) - \beta_2 (x_{20}^3 \\ & -3x_{20}^2 x_{10} + 3x_{20}x_{10}^2 - x_{10}^3) - \zeta_4 (D_0 x_{20} - D_0 x_{10})\end{aligned} \tag{9}$$

The general solution of equations (6)-(7) can be expressed in the form

$$x_{10} = A_1 e^{i\omega_1 T_0} + cc \tag{10}$$

$$x_{20} = A_2 e^{i\omega_2 T_0} + A_1 \left[\omega_2^2 / (\omega_2^2 - \omega_1^2)\right] e^{i\omega_1 T_0} + cc \tag{11}$$

where $A_1$ and $A_2$ are unknown functions in $T_1$, which can be determined from eliminating the secular terms at the next approximation, and *cc* stands for the conjugate of the preceding terms. The particular solutions of equations (8)-(9) after eliminating the secular terms are given by:

$$x_{11} = U_1 e^{i\Omega_1 T_0} + U_2 e^{i(\Omega_2+\omega_1)T_0} + U_3 e^{i(\Omega_2-\omega_1)T_0} + H_1 e^{2i\omega_1 T_0} + H_2 e^{3i\omega_1 T_0}$$
$$+ H_3 e^{i\omega_2 T_0} + H_4 e^{2i\omega_2 T_0} + H_5 e^{3i\omega_2 T_0} + H_6 e^{i(\omega_1+\omega_2)T_0} + H_7 e^{i(\omega_1-\omega_2)T_0}$$
$$+ H_8 e^{i(2\omega_1+\omega_2)T_0} + H_9 e^{i(2\omega_1-\omega_2)T_0} + H_{10} e^{i(\omega_1+2\omega_2)T_0} + H_{11} e^{i(\omega_1-2\omega_2)T_0} + H_{12} + cc \quad (12)$$

$$x_{21} = U_4 e^{i\Omega_1 T_0} + U_5 e^{i(\Omega_2+\omega_1)T_0} + U_6 e^{i(\Omega_2-\omega_1)T_0} + H_{13} e^{i\omega_1 T_0} + H_{14} e^{2i\omega_1 T_0}$$
$$+ H_{15} e^{3i\omega_1 T_0} + H_{16} e^{2i\omega_2 T_0} + H_{17} e^{3i\omega_2 T_0} + H_{18} e^{i(\omega_1+\omega_2)T_0} + H_{19} e^{i(\omega_1-\omega_2)T_0}$$
$$+ H_{20} e^{i(2\omega_1+\omega_2)T_0} + H_{21} e^{i(2\omega_1-\omega_2)T_0} + H_{22} e^{i(\omega_1+2\omega_2)T_0}$$
$$+ H_{23} e^{i(\omega_1-2\omega_2)T_0} + H_{24} + cc \quad (13)$$

where $U_i$, $i$=1 to 6 , $H_i$, $i$=1 to 24, are complex functions in $T_1$. The general solution of $x_1$ and $x_2$ up to the first-order approximation is given by

$$x_1 = x_{10} + \varepsilon x_{11} + \ldots \quad , \quad x_2 = x_{20} + \varepsilon x_{21} + \ldots$$

### 3.2. Resonance Cases

From the equations (10) to (13) all possible resonance cases are:

(a) Trivial resonance: $\Omega_j \cong \omega_j = 0$, $j$ =1,2. (b) Internal resonance: $\omega_1 \cong n\omega_2$, $\omega_2 \cong n\omega_1$ , $n$ =1,2,3 (c) Primary resonance: $\Omega_1 \cong \omega_1$ , $\Omega_1 \cong \omega_2$

(d) Sub-harmonic resonance: $\Omega_2 \cong 2\omega_1$ (e) Combined resonance: $\Omega_2 \cong \pm\omega_1 \pm \omega_2$

(f) Simultaneous resonance: Any combination of the above resonance cases is considered as simultaneous resonance

### 3.3. Stability Analysis

The stability of the system is investigated at one of the worst resonance cases (confirmed numerically), which is the simultaneous primary, principal parametric and internal resonance where $\Omega_1 \cong \omega_1$, $\Omega_2 \cong 2\omega_1$ and $\omega_2 \cong 3\omega_1$. Using the detuning parameters $\sigma_1$, $\sigma_2$ and $\sigma_3$ such that:

$$\Omega_1 = \omega_1 + \varepsilon\sigma_1 \quad , \Omega_2 = 2\omega_1 + \varepsilon\sigma_2 \quad \text{and} \quad \omega_2 = 3\omega_1 + \varepsilon\sigma_3 \quad (14)$$

Substituting equation (14) into equations (8)-(9) and eliminating the secular terms leads to the solvability conditions as

$$2i\omega_1 D_1 A_1 = \left[-i\omega_1\zeta_1 + \alpha_3\Gamma - i\omega_1\zeta_3(1-\Gamma)\right]A_1 - \left[i\omega_1\zeta_2 + 3\alpha_2 + 3\alpha_5(1-\Gamma)^3\right]A_1^2\bar{A}_1$$
$$-6\alpha_5(1-\Gamma)A_1A_2\bar{A}_2 + \frac{F_1}{2}e^{i\sigma_1 T_1} + \frac{\bar{A}_1 F_2}{2}e^{i\sigma_2 T_1} + 3\alpha_5(1-\Gamma)^2\bar{A}_1^2 A_2 e^{i\sigma_3 T_1} \quad (15)$$

$$2i\omega_2 D_1 A_2 = -i\omega_2\zeta_4 A_2 + \left[\omega_2^2\Gamma_1 + \beta_2(1-\Gamma)^3\right]A_1^3 e^{-i\sigma_3 T_1} + \omega_2^2\Gamma_2 A_2$$
$$-3\beta_2 A_2^2\bar{A}_2 - 6\beta_2(1-\Gamma)^2 A_1\bar{A}_1 A_2 \quad (16)$$

where $\Gamma = \omega_2^2/(\omega_2^2-\omega_1^2)$ , $\Gamma_1 = \left[i\omega_1\zeta_2 + \alpha_2^2 + \alpha_5(1-\Gamma)^3\right]/8\omega_1^2$

and $\Gamma_2 = \left[ i\omega_2\zeta_3 + \alpha_3 + 6\alpha_5 A_1\bar{A}_1(1-\Gamma)^2 + 3\alpha_5 A_2\bar{A}_2 \right] / (\omega_1^2 - \omega_2^2)$

We express the complex function $A_n$ in the polar form as

$$A_n = (1/2)a_n(T_1)e^{i\mu_n(T_1)} \qquad (n=1,2) \tag{17}$$

where $a_n$ and $\mu_n$ are real. Substituting equation (17) into equations (15) and (16) and separating real and imaginary part yields,

$$a_1' = \frac{F_1}{2\omega_1}\sin\gamma_1 + \left[\frac{F_2}{4\omega_1}\sin\gamma_2 - \frac{\zeta_1+\zeta_3(1-\Gamma)}{2}\right]a_1 + \left[\frac{3\alpha_5(1-\Gamma)^2}{8\omega_1}\sin\gamma_3\right]a_1^2a_2 - \frac{\zeta_2}{8}a_1^3 \tag{18}$$

$$\mu_1'a_1 = -\frac{F_1}{2\omega_1}\cos\gamma_1 - \left[\frac{F_2}{4\omega_1}\cos\gamma_2 + \frac{\alpha_3\Gamma}{2\omega_1}\right]a_1 + \left[\frac{3\alpha_5(1-\Gamma)}{4\omega_1}\right]a_1a_2^2 - \left[\frac{3\alpha_5(1-\Gamma)^2}{8\omega_1}\cos\gamma_3\right]a_1^2a_2$$
$$+3\left[\frac{\alpha_2+\alpha_5(1-\Gamma)^3}{8\omega_1}\right]a_1^3 \tag{19}$$

$$a_2' = -\left[\frac{\zeta_3\Gamma+\zeta_4}{2}\right]a_2 - \left[\Gamma_3\sin\gamma_3 - \frac{\omega_2\zeta_2}{64\omega_1}\cos\gamma_3\right]a_1^3 \tag{20}$$

$$\mu_2'a_2 = \frac{\alpha_3\Gamma}{2\omega_2}a_2 + \left[\frac{3(\alpha_5\Gamma+\beta_2)(1-\Gamma)^2}{4\omega_2}\right]a_1^2a_2 + \left[\frac{3(\alpha_5\Gamma+\beta_2)}{8\omega_2}\right]a_2^3 - \left[\Gamma_3\cos\gamma_3 + \frac{\omega_2\zeta_2}{64\omega_1}\sin\gamma_3\right]a_1^3 \tag{21}$$

where $$\Gamma_3 = \left[\frac{\omega_2(\alpha_2+\alpha_5(1-\Gamma)^3)}{64\omega_1^2} + \frac{\beta_2(1-\Gamma)^3}{8\omega_2}\right]$$

and $\gamma_1 = \sigma_1T_1 - \mu_1, \gamma_2 = \sigma_2T_1 - 2\mu_1, \gamma_3 = \sigma_3T_1 - 3\mu_1 + \mu_2$ (22)

For the steady state solution $a_n' = \gamma_n' = 0$. Then from equation (22) yields

$$\mu_1' = \sigma_1 = \sigma_2/2 = \sigma \quad , \quad \mu_2' = 3\sigma - \sigma_3 \tag{23}$$

Then it follows from equations (18)-(21) that the steady state solutions are given by

$$\frac{F_1}{2\omega_1}\sin\gamma_1 + \left[\frac{F_2}{4\omega_1}\sin\gamma_2 - \frac{\zeta_1+\zeta_3(1-\Gamma)}{2}\right]a_1 + \left[\frac{3\alpha_5(1-\Gamma)^2}{8\omega_1}\sin\gamma_3\right]a_1^2a_2 - \frac{\zeta_2}{8}a_1^3 = 0 \tag{24}$$

$$a_1\sigma + \frac{F_1}{2\omega_1}\cos\gamma_1 + \left[\frac{F_2}{4\omega_1}\cos\gamma_2 + \frac{\alpha_3\Gamma}{2\omega_1}\right]a_1 - \left[\frac{3\alpha_5(1-\Gamma)}{4\omega_1}\right]a_1a_2^2 + \left[\frac{3\alpha_5(1-\Gamma)^2}{8\omega_1}\cos\gamma_3\right]a_1^2a_2$$
$$-\left\{[3\alpha_2 + 3\alpha_5(1-\Gamma)^3]/8\omega_1\right\}a_1^3 = 0 \tag{25}$$

$$-\left[(\zeta_3\Gamma+\zeta_4)/2\right]a_2 - \left[\Gamma_3\sin\gamma_3 - (\omega_2\zeta_2/64\omega_1)\cos\gamma_3\right]a_1^3 = 0 \tag{26}$$

$$a_2(3\sigma-\sigma_3) - \frac{\alpha_3\Gamma}{2\omega_2}a_2 - \left[\frac{3(\alpha_5\Gamma+\beta_2)(1-\Gamma)^2}{4\omega_2}\right]a_1^2a_2 - \left[\frac{3(\alpha_5\Gamma+\beta_2)}{8\omega_2}\right]a_2^3$$
$$+\left[\Gamma_3\cos\gamma_3 + (\omega_2\zeta_2/64\omega_1)\sin\gamma_3\right]a_1^3 = 0 \tag{27}$$

Solving the resulting algebraic equations yields two possibilities for the fixed points for each case.

**Case (1):** The controller is deactivated ( $a_1 \neq 0, a_2 = 0$), the frequency response equation can be obtained in the form

$$\left\{\frac{9\alpha_2^2}{64\omega_1^2}\right\}a_1^6 - \left\{\frac{3\sigma\alpha_2}{4\omega_1}\right\}a_1^4 + \left\{\sigma^2 + \frac{\zeta_1^2}{4}\right\}a_1^2 - \frac{F_1^2}{4\omega_1^2} - \frac{F_2^2}{16\omega_1^2}a_1^2 - \frac{F_1F_2}{4\omega_1^2}a_1\cos(\gamma_1-\gamma_2) = 0 \quad (28)$$

**Case (2):** the controller is activated ($a_1 \neq 0, a_2 \neq 0$), the resulting two equations are obtained

$$\Gamma_4 a_1^6 + \Gamma_5 a_1^4 + \Gamma_6 a_1^2 + \Gamma_7 a_1^4 a_2^2 + \Gamma_8 a_1^2 a_2^4 + \Gamma_9 a_1^2 a_2^2 + \Gamma_{10} a_1^2 a_2 - \frac{F_1^{\,2}}{4\omega_1^2} - \frac{F_2^{\,2}}{16\omega_1^2}a_1^2 - (F_1F_2/4\omega_1^2)a_1\cos(\gamma_1-\gamma_2) = 0 \quad (29)$$

$$\Gamma_{11} a_2^6 + \Gamma_{12} a_2^4 + \Gamma_{13} a_2^2 + \Gamma_{14} a_2^4 a_1^2 + \Gamma_{15} a_2^2 a_1^2 + \Gamma_{16} a_1^4 a_2^2 + \Gamma_{17} a_1^6 = 0 \quad (30)$$

where $\Gamma_i\,(i = 4,...,17)$ are given in the appendix.

## 4. Numerical Results and Discussion

To study the behavior of the main system, the Runge-Kutta fourth-order method was applied to the equation (1) governing the oscillating system, after eliminating all parameters corresponding to controller. Fig. 2 shows the steady state amplitude and phase plane of the main system at the primary resonance where $\Omega_1 \cong \omega_1$ for the parameters $\zeta_1 = 0.05,\ F_1 = 0.6, F_2 = 0.3, \alpha_1 = 0.03, \alpha_2 = 0.04$. In this Figure, we observe that the steady state amplitude is about five of the excitation force amplitude $F_1$. The main system is stable.

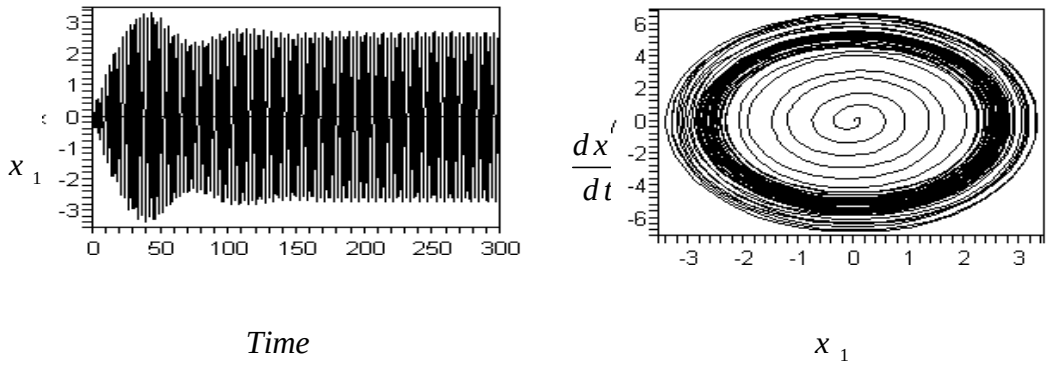


Fig. 2. System behavior without absorber at primary resonance $\Omega_1 \cong \omega_1$ and $\Omega_2$ is a way from $\omega_1$.

Figs. 3 and 4 show the steady state amplitude and phase plane of the main system at the principle parametric and simultaneous primary and principle parametric resonance respectively where $\Omega_2 \cong 2\omega_1$ and $\Omega_1 \cong \omega_1$, $\Omega_2 \cong 2\omega_1$. In these Figures, we note that the steady state amplitude is about 9 and 6 of the excitation force amplitude $F_1$ respectively. Also the chaotic wave motion will increase.

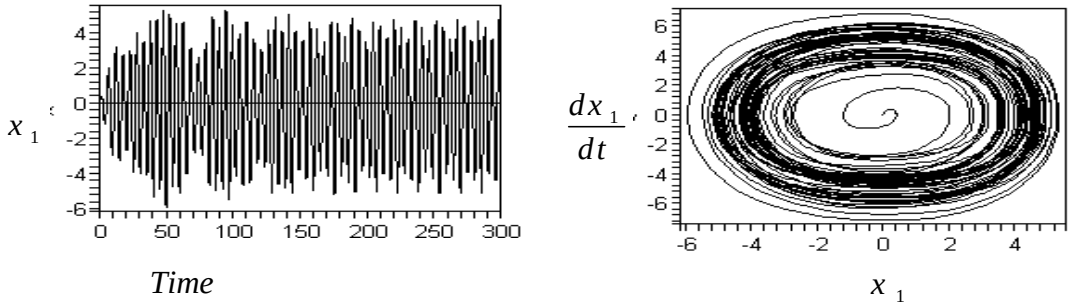


Fig. 3. System behavior without absorber at principle parametric resonance $\Omega_2 \cong 2\omega_1$ and $\Omega_1$ is a way from $\omega_1$.

Fig. 5 shows that the steady state amplitude of the system with absorber at the simultaneous primary and internal resonance $\Omega_1 \cong \omega_1, \omega_2 \cong 3\omega_1$. The effectiveness of the absorber $E_a$ ($E_a$ = steady state amplitude of the system without absorber / steady state amplitude of the system with absorber) is about 5, which means that the steady state amplitude is reduced to less than 20 % of the maximum amplitude shown in Fig. 2.

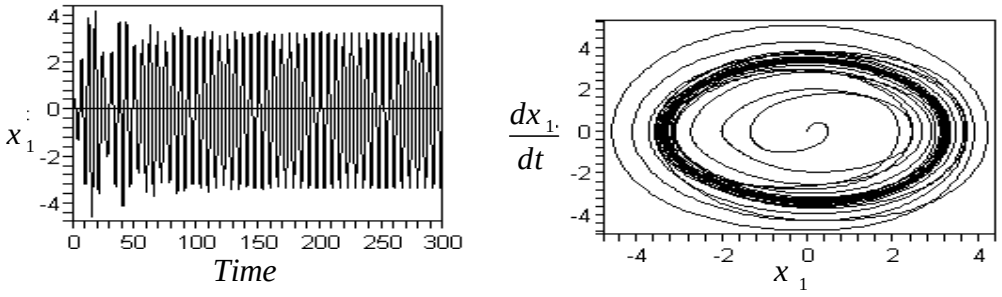


Fig. 4. System behavior without absorber at simultaneous resonance $\Omega_1 \cong \omega_1$ and $\Omega_2 \cong 2\omega_1$.

Also, the oscillations of the system and absorber have multi-limit cycle and chaotic, respectively. All solutions of the system and absorber are stable. Fig. 6 shows that the steady state amplitude of the system with absorber at the simultaneous principal parametric and internal resonance $\Omega_2 \cong 2\omega_1, \omega_2 \cong 3\omega_1$. The effectiveness of the absorber $E_a$ is about 10, which means that the steady state amplitude is reduced to less than 10 % of the maximum amplitude shown in Fig. 3. Also, the oscillations of the system and absorber have multi-limit cycle and increasing dynamic chaos, respectively.

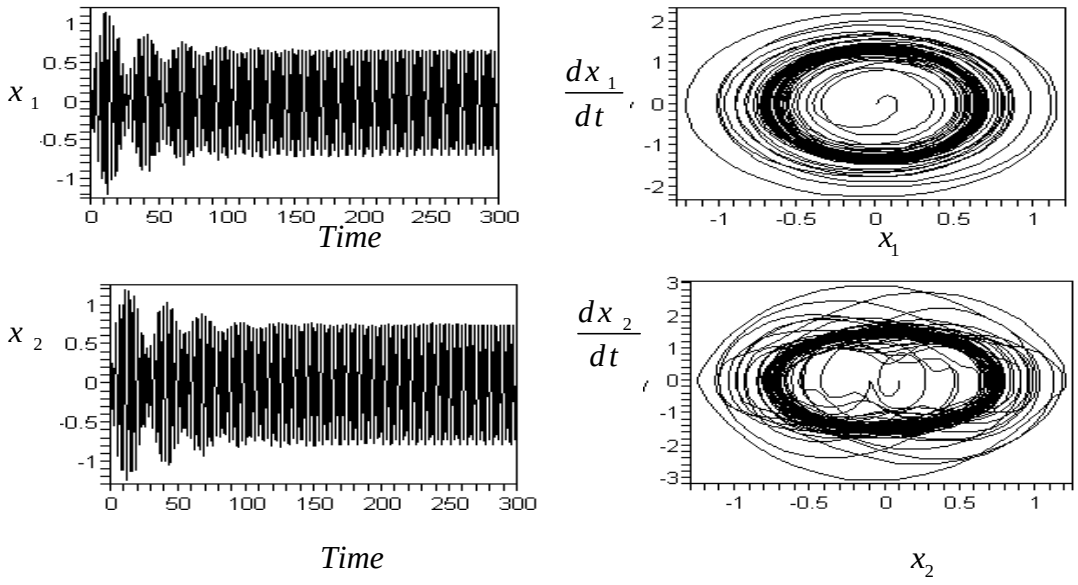


Fig.5. Response of the system and absorber at simultaneous resonance $\Omega_1 \cong \omega_1$ and $\omega_2 \cong 3\omega_1$.

Fig. 7 shows that the steady state amplitude of the system with absorber at the simultaneous resonance $\Omega_1 \cong \omega_1, \Omega_2 \cong 2\omega_1$ and $\omega_2 \cong 3\omega_1$. The effectiveness of the absorber $E_a$ is about 7, which means that the steady state amplitude is reduced to less than 14 % of the maximum amplitude shown in Fig. 4. Also, the oscillations of the system and absorber have multi-limit cycle and increasing dynamic chaos, respectively.

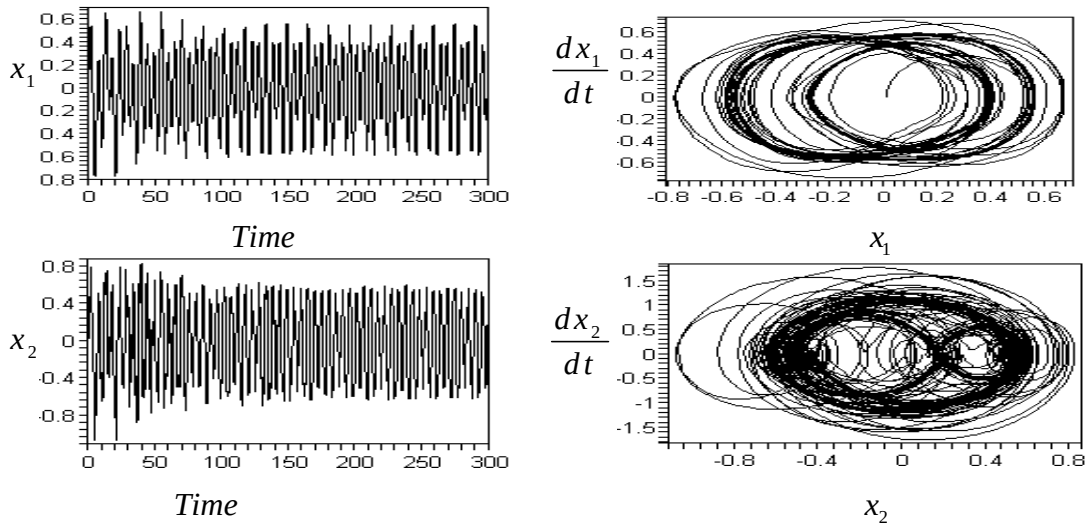


Fig.6. Response of the system and absorber at simultaneous resonance $\Omega_2 \cong 2\omega_1$ and $\omega_2 \cong 3\omega_1$.

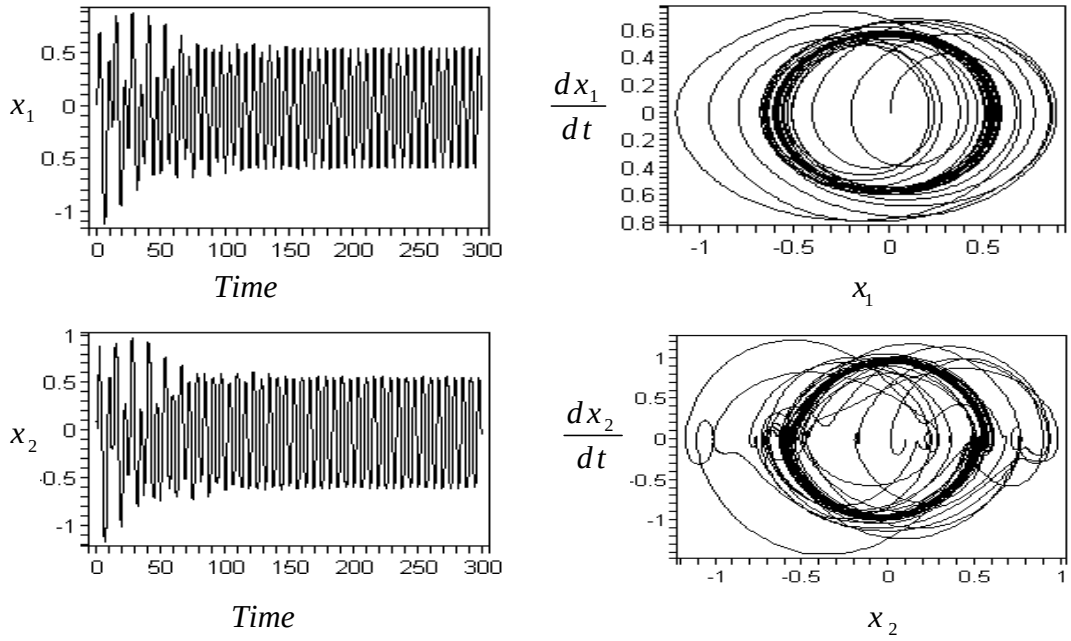


Fig.7. Response of the system and absorber at simultaneous resonance $\Omega_1 \cong \omega_1$, $\Omega_2 \cong 2\omega_1$ and $\omega_2 \cong 3\omega_1$.

### 4.2 Theoretical frequency and force-response curves

**Case 1 : The controller is deactivated,** $a_1 \neq 0, a_2 = 0$**:**

The analytical analysis is represented graphically by using the numerical methods. The frequency response equation (28) is a nonlinear algebraic equation, which are solved numerically by using Newton Raphson method. The numerical results are shown in Figures 8-17. In all Figures, the region of stability of non-trivial solutions is determined by applying the Routh-Hurwitz criterion. The stable and unstable solutions are represented by solid and dotted lines respectively on the response curves. Figs 8-17 show the frequency-response and force-response curves for the stability first case. In Figs. 8-12, we observe that the solutions is stable for negative values of $\sigma_1$ and it has stable and unstable for positive values of $\sigma_1$. Fig. 8 shows the effects of he detuning parameter $\sigma_1$ on the steady state amplitude of the system. In this Figure, the response amplitude consists of a continuous curve which is bent to the right and has hardening phenomena. This continuous curve has stable and unstable solutions.

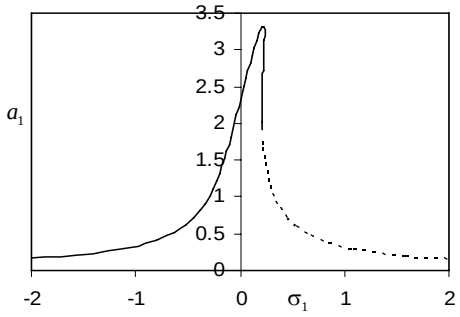


Fig. 8. Effects of the detuning parameter $\sigma_1$

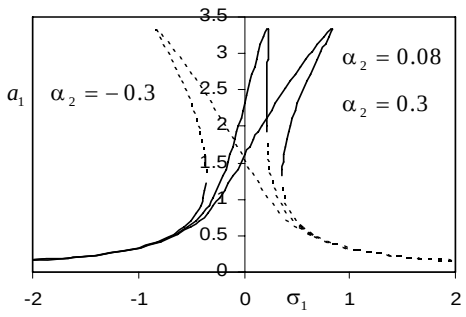


Fig. 9. Effects of the nonlinear spring stiffness $\alpha_2$

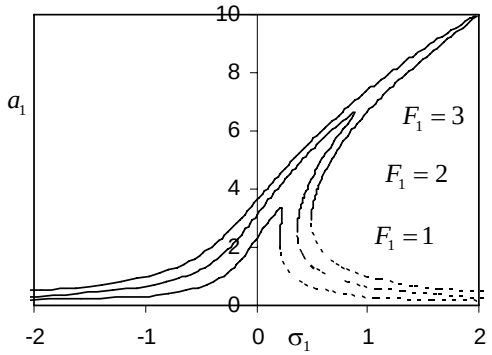


Fig. 10. Effects of the excitation amplitude $F_1$

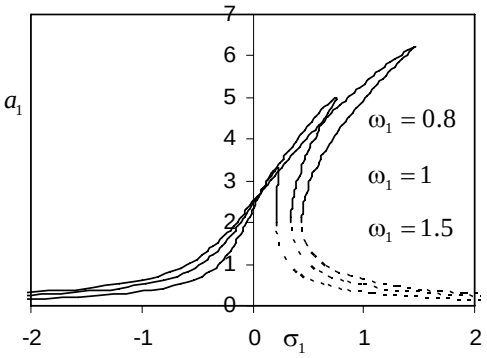


Fig. 11. Effects of the natural frequencies

Fig. 9 shows that as non-linear spring stiffness $\alpha_2$ is increased positively the continuous curve is moved downwards and has decreased magnitudes. It can be concluded that increasing the non-linear spring stiffness $\alpha_2$ can reduce the amplitude of the system and obtain the effect of reduction of the vibration amplitude. The regions of multi-valued and instability zone are increased and decreased respectively. Also for negative value of non-linear spring stiffness $\alpha_2$ the response amplitude is bent to the left and the stability region is decreased. The positive and negative values of the non-linear spring stiffness $\alpha_2$ produce either hard or soft spring, respectively. The steady state amplitude $a_1$ is a monotonic increasing function in the excitation amplitude $F_1$ and for small values of $F_1$ the single-valued curve is shifted upwards with decreased instability zone, as shown in Fig. 10. The zones of multi-valued and instability region are increased for large values of $F_1$. It is clear that from Fig. 11 for decreasing natural frequency $\omega_1$ the steady state amplitude is increasing and the curve is bent to the right, leading to multi-valued amplitudes and to appearance of the jump phenomenon. From Fig. 12, the steady state amplitude is a monotonic decreasing function in the damping coefficient $\zeta_1$. When the linear damping factor $\zeta_1$ increase up to 0.2, we note that the bending contracts with decreased magnitudes and the multi-valued disappears.

Figs. 13-17 represent the external excitation-response curves for primary resonance. It is evident from Fig. 13 that the response amplitude has a continuous curve and there exist zone of multi-valued solutions. There exist jump phenomenon and the curve has unstable and stable solutions. From Fig. 14, we observe that for increasing positive value of non-linear spring stiffness $\alpha_2$ the continuous curve is shifted downwards with decreasing region of instability. For negative values of $\alpha_2$, the continuous curve becomes unstable and the region of multi-valued is disappeared. Figs. 15 and 16 show that for increasing values of natural frequency $\omega_1$ and detuning parameter $\sigma_1$, respectively, the curve is shifted upwards and has increased instability region. The region of multi-valued is increased for increased natural frequency, detuning parameters. For negative value of detuning parameter $\sigma_1$, the continuous curve becomes stable and the region of multi-valued is disappeared as shown in Fig. 16. For increasing value of damping coefficient $\zeta_1$, we note that the region of multi-valued is disappeared and the continuous curve has a single valued curve which is shifted downwards with increasing instability zone as shown in Fig. 17.

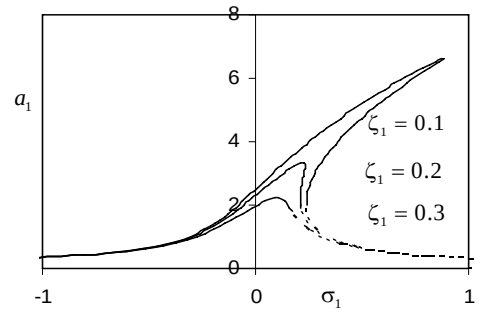


Fig.12. Effects of the damping coefficient $\zeta_1$

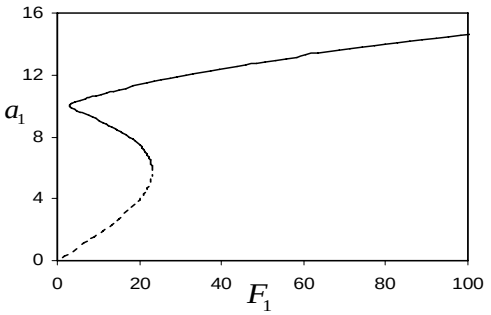


Fig.13. Excitation-response curve of $\Omega_1 \cong \omega_1$

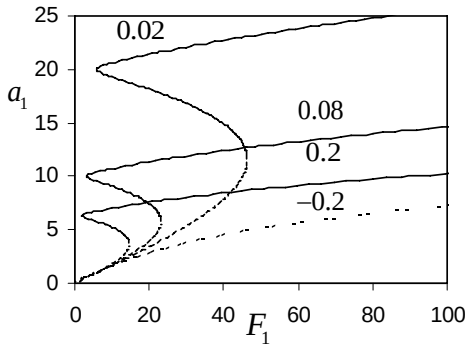


Fig. 14. Effects of the non-linear spring stiffness $\alpha_2$

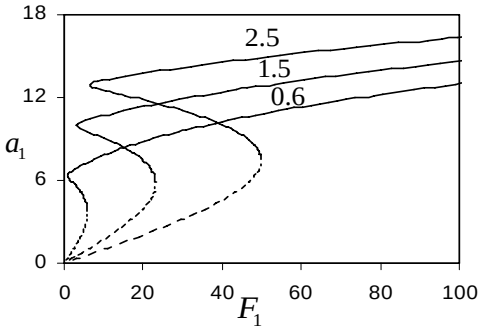


Fig.15. Effects of the natural frequency $\omega_1$

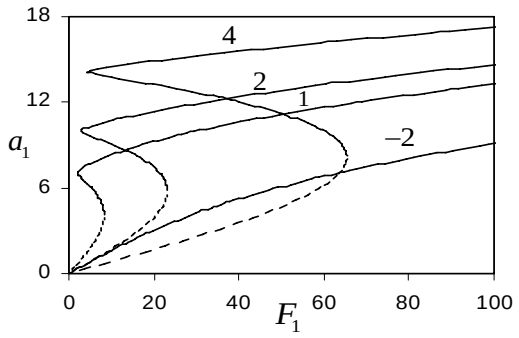


Fig.16. Effects of the detuning parameter $\sigma_1$

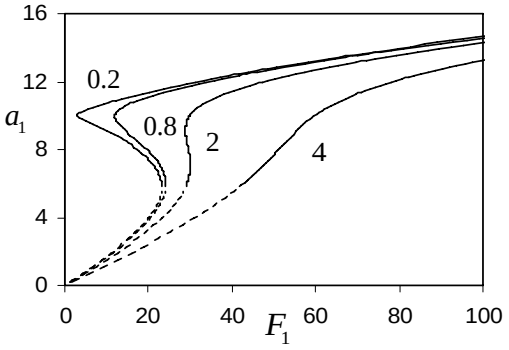


Fig.17. Effects of the damping coefficient $\zeta_1$

**Case 2 : The controller is activated,** $a_1 \neq 0, a_2 \neq 0$**:**

The frequency response equations (29) and (30) are nonlinear algebraic equations, which are solved numerically. The numerical results are shown in Figures 18-22. The solid curves denote the stable solutions and the dotted curves denote the unstable solutions. These Figures, show the steady state response-frequency curve for the stability second case, where $a_1, a_2 \neq 0$ in the case of simultaneous primary resonance in the presence of three-to-one internal resonance. In these Figures, we observe that the solutions is stable for negative values of $\sigma_1$ and it has stable and unstable for positive values of $\sigma_1$. Fig. 18 shows that the effect of the detuning parameter $\sigma_1$ on the steady state amplitudes of the system and absorber. In this Figure, we observe that, the amplitudes $a_1$ and $a_2$ have one continuous curve, that the continuous curve of the system lies upper than the continuous curve of the absorber. For increasing excitation force $F_1$, we note that the stability magnitudes of the system and absorber are increased as shown in Fig. 19.

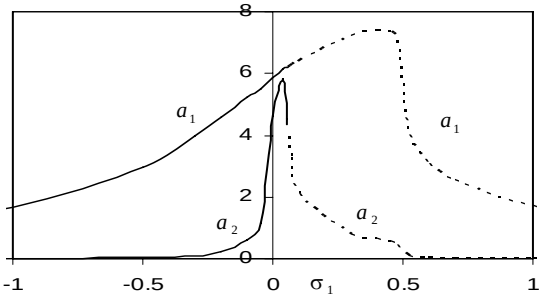


Fig.18. Effects of the detuning parameter $\sigma_1$

Several groups of various parameters are tried out to discuss the vibration property of the system and the selections of the relative parameters are taken by virtue of Ref. [10].

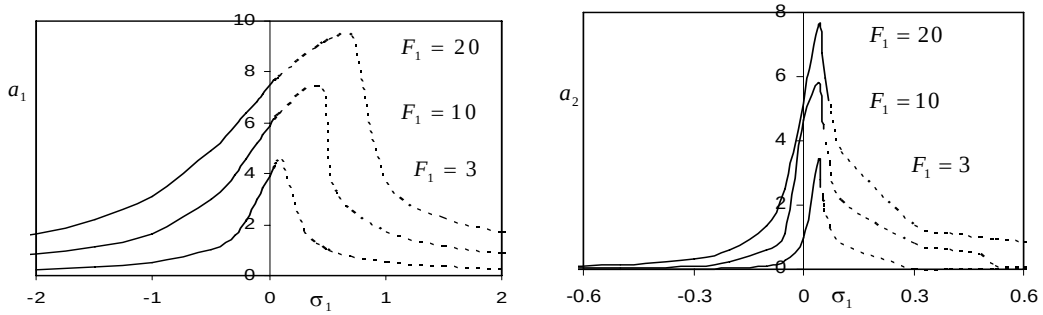


Fig. 19. Effects of the excitation amplitude $F_1$

In Fig. 20, with increase in the non-linear spring stiffness $\alpha_2$, the vibration amplitude of the system and absorber reduces. It can be concluded that increasing the non-linear spring stiffness $\alpha_2$ can reduce the amplitude of the main mass and obtain the effect of reduction of the vibration amplitude. The system and absorber becomes unstable for negative value of non-linear spring stiffness $\alpha_2$. Fig. 21 shows that for increasing linear damping coefficient, we observe that the both system and absorber have decreasing magnitudes. Fig. 22 evaluates the effectiveness of the cubic non-linear damping $\zeta_2$ on the amplitude reduction of the system. From the curves, it can be seen that the non-linear damping has an obvious effect on the amplitude reduction.

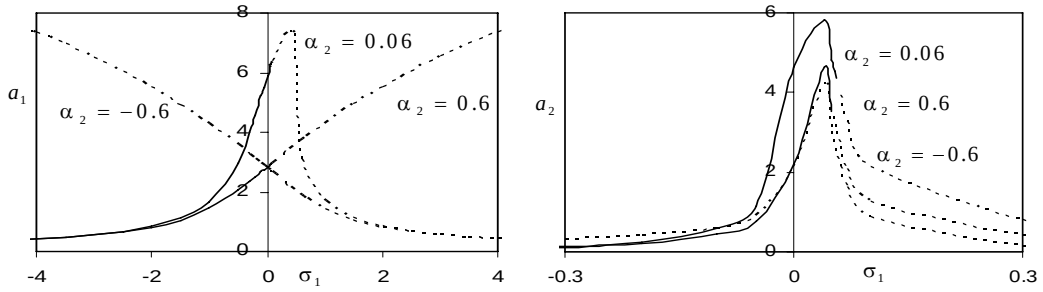


Fig. 20. Effects of the non-linear parameter $\alpha_2$

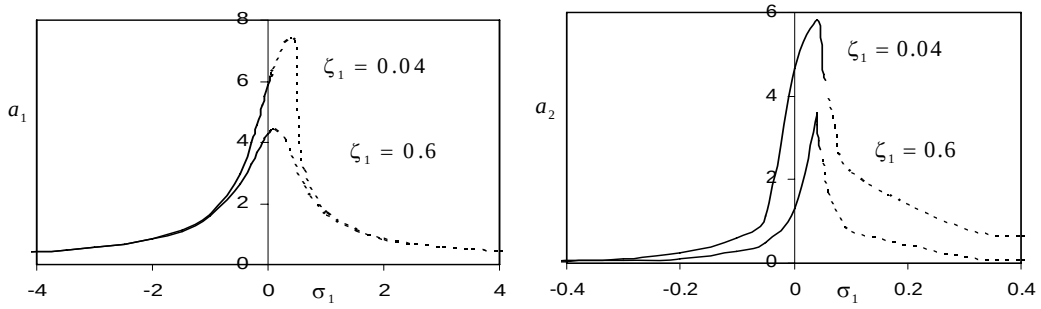


Fig. 21. Effects of the linear damping coefficient $\zeta_1$

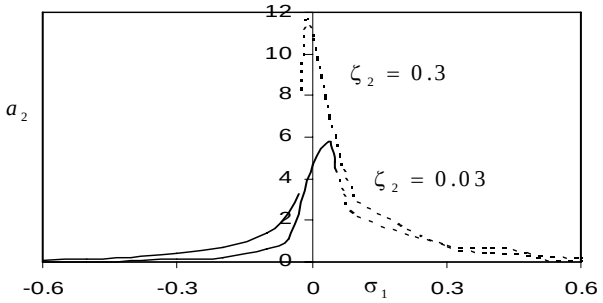


Fig. 22. Effects of the cubic non-linear damping $\zeta_2$

## 5. Conclusions

The system consists of the main system and the absorber representing the vibration of many applications in machine tools, ultrasonic cutting process, subjected to external and parametric excitation forces is considered and solved using the method of multiple scale perturbation. A simple and powerful effective method is demonstrated to reduce (control passively) both vibration and dynamic chaos in the non-linear system using non-linear absorber. One of the most common methods of vibration control is the dynamic absorber. Multiple scales perturbation technique is applied to determine approximate solutions of the coupled non-linear differential equations. Steady state solutions and their stability are studied for selected values of different parameters. Frequency response equations are deduced to investigate system stability. It can be seen from the results that the optimal working conditions of the system is principle parametric and internal resonance $\Omega_2 \cong 2\omega_1, \omega_2 \cong 3\omega_1$. From the above study the following may be concluded.

**(i) When the controller is deactivated**

1. The steady state amplitude is a monotonic increasing and decreasing function to the excitation amplitudes $F_1$ , $F_2$ and natural frequency $\omega_1$ , damping coefficient $\zeta_1$ , respectively.

2. The zones of multi-valued and instability region are increased for large values of $F_1$.
3. For increasing positive value of non-linear spring stiffness $\alpha_2$ the continuous curve is shifted downwards produce hard spring with decreasing region of instability.
4. For negative values of $\alpha_2$, the curve is bent to the left produce soft spring, the region of unstable is increased and the region of multi-valued is disappeared.
5. The region of multi-valued is disappeared for increasing value of damping coefficient $\zeta_1$, and the continuous curve has a single valued curve which is shifted downwards.
6. The continuous curve becomes stable and the region of multi-valued is disappeared for negative value of detuning parameter $\sigma_1$.
7.

**(ii) When the controller is activated**

1. The optimum working conditions for the system are when, $\Omega_2 \cong 2\omega_1$, $\omega_2 \cong 3\omega_1$ since the steady state amplitude of the system is reduced to 10 % of its maximum value. This means that the effectiveness of the absorber $E_a$ = 10.
2. The effectiveness of the absorber $E_a$ is about 5 and 7 for simultaneous primary and internal resonance $\Omega_1 \cong \omega_1$, $\omega_2 \cong 3\omega_1$ and simultaneous resonance $\Omega_1 \cong \omega_1$, $\Omega_2 \cong 2\omega_1$, $\omega_2 \cong 3\omega_1$ respectively.
3. For increasing excitation force $F_1$ and decreasing damping coefficient, we note that the stability magnitudes of the main system and absorber are increased.
4. From the curves, it can be seen that the non-linear damping has an obvious effect on the amplitude reduction of the system, which is a good agreement with Ref. [14].
5. Increasing the non-linear spring stiffness $\alpha_2$ can reduce the amplitude of the main mass and obtain the effect of reduction of the vibration amplitude, which is a good agreement with Ref. [14].
6. Numerical simulations show the system exhibits periodic motions and chaotic motions, which is a good agreement with Ref. [14].

In comparison with the previous work [14] the authors consider the nonlinear dynamic and spring as a cubic one only. The method of averaging is used to obtain the steady state response and the system is subjected to single external excitation force. The stability is studied applying bifurcation and Poincare` map. It is worth to mention that in the reported results assuming the nonlinear term is zero. In our study, the model considered in Ref. [14], but subjected to external and parametric excitation forces instead of an external only.

## Appendix

$$\Gamma_4 = \frac{\zeta_2^2}{64} + \left[\frac{3\alpha_2 + 3\alpha_5(1-\Gamma)^3}{8\omega_1}\right]^2 \qquad \Gamma_5 = \left[\zeta_1 + \zeta_3(1-\Gamma)\right]\left\{\frac{\zeta_2}{8}\right\} - \left[\frac{3\alpha_2 + 3\alpha_5(1-\Gamma)^3}{8\omega_1}\right](\sigma + \frac{\alpha_3\Gamma}{2\omega_1}$$

$$\Gamma_6 = \left[\frac{\zeta_1 + \zeta_3(1-\Gamma)}{2}\right]^2 + \left[\sigma + \frac{\alpha_3\Gamma}{2\omega_1}\right]^2, \qquad \Gamma_7 = \frac{9\alpha_5^2(1-\Gamma)^4}{64\omega_1^2} + \left[\frac{3\alpha_2 + 3\alpha_5(1-\Gamma)^3}{8\omega_1}\right]\frac{3\alpha_5(1-\Gamma)}{2\omega_1}$$

$$\Gamma_8 = \left[\frac{3\alpha_5(1-\Gamma)}{4\omega_1}\right]^2, \qquad \Gamma_9 = -\left[\frac{3\alpha_5(1-\Gamma)}{2\omega_1}\right]\left[\sigma + \frac{\alpha_3\Gamma}{2\omega_1}\right]$$

$$\Gamma_{10} = \left[\frac{3\alpha_5(1-\Gamma)^2 F_1}{16\omega_1^2}\right]\cos(\gamma_1 - \quad , \quad \Gamma_{11} = \left[\frac{3(\alpha_5\Gamma + \beta_2)}{8\omega_2}\right]^2$$

$$\Gamma_{12} = \left[3\sigma - \sigma_3 - \frac{\alpha_3\Gamma}{2\omega_2}\right]\frac{3(\alpha_5\Gamma + \beta}{4\omega_2}, \quad \Gamma_{13} = \left[\frac{\zeta_3\Gamma + \zeta_4}{2}\right]^2 + \left[3\sigma - \sigma_3 - \frac{\alpha_3\Gamma}{2\omega_2}\right]^2$$

$$\Gamma_{14} = \left[\frac{3(\alpha_5\Gamma + \beta_2)(1-\Gamma)}{4\omega_2}\right]^2, \qquad \Gamma_{16} = (1-\Gamma)^2\,\Gamma_{14}, \; \Gamma_{17} = -\left[\Gamma_3^2 + \frac{\omega_2^2\zeta_2^2}{(64\omega_1)^2}\right]$$

## References


1. Oueini SS., Nayfeh AH., “Single-Mode control of a cantilever beam under principal parametric excitation”, Journal of Sound and Vibration 224(1) (1999) 33-47.
2. Asfar KR., “Effect of non-linearities in elastomeric material dampers on torsional vibration control”, International Journal of Non-linear Mechanics 27(6) (1992) 947–54.
3. Eissa M., “Vibration Control of Non-linear Mechanical Systems Via Neutralizers”, Electronic Engineering Bulletin, No. 18, July 1999, Egypt.
4. Eissa M., “Vibration and chaos control in I.C engines subject to harmonic torque via non-linear absorbers”, In. Proc of ISMV Conference, Islamabad, Pakistan, 2000.
5. Eissa M., El-Ganaini W., “Part I, Multi-absorbers for vibration control of non-linear structures to harmonic excitations”, In. Proc of ISMV Conference, Islamabad, Pakistan, 2000.
6. Eissa M., El-Ganaini W., “Part II, Multi-absorbers for vibration control of non-linear structures to harmonic excitations”, In. Proc of ISMV Conference, Islamabad, Pakistan, 2000.
7. Kamel MM., Amer YA., “Response of parametrically excited one-degree-of-freedom system with non-linear damping and stiffness”, Physica Scripta 66 (2002) 410–416.

8. Song Y., Sato H., Iwata Y. and Komatsuzaki T., "The response of a dynamic vibration absorber system with a parametrically excited pendulum", Journal of Sound and Vibration 259(4) (2003) 747-759.
9. Soom A., Lee M., "Optimal design of linear and non-linear vibration absorbers for damped system", Journal of Vibration, Acoustic Stress, and Reliability in Design 105 (1983) 112-119.
10. Jordanov IN., Cheshankov BI., "Optimal design of linear and non-linear dynamic vibration absorbers", Journal of Sound and Vibration 123(1) (1988) 157-170.
11. Rice H.J., "Combinational instability of the non-linear vibration absorber", Journal of Sound and Vibration 108(4) (1986) 5 26-532.
12. Shaw J., Shaw SW., Haddow AG., "On the response of the non-linear vibration absorber", Journal of Non-linear Mechanics 24 (1989) 281-293.
13. Natsiavas S., "Steady state oscillations and stability of non-linear dynamic vibration absorbers", Journal of Sound and Vibration 156(2) (1992) 227-245.
14. Zhu SJ., Zheng YF., Fu YM., "Analysis of non-linear dynamics of a two-degree-of-freedom vibration system with non-linear damping and non-linear spring", Journal of Sound and Vibration 271 (2004) 15-24.
15. Lim FCN., Cartmell MP., Cardoni A., Lucas M., "A preliminary investigation into optimizing the response of vibrating systems used for ultrasonic cutting", Journal of Sound and Vibration 272 (2004) 1047-1069.
16. Eissa M., Amer YA., "Vibration control of a cantilever beam subject to both external and parametric excitation", Applied Mathematics and Computation 152 (2004) 611-619.
17. Nayfeh AH., "Resolving Controversies in the Application of the Method of Multiple Scales and the Generalized Method of Averaging", Nonlinear Dynamics 40 (2005) 61-102.
18. El-bassiouny AF., "Effect of non-linearities in elastomeric material dampers on torsional oscillation control", Applied Mathematics and Computation 162 (2005) 835-854.
19. Eissa M., Sayed M., "A Comparison between active and passive vibration control of non-linear simple pendulum, Part I: Transversally tuned absorber and negative $G\dot{\varphi}^n$ feedback", Mathematical and Computational Applications 11(2) (2006) 137-149.
20. Eissa M., Sayed M., "A Comparison between active and passive vibration control of non-linear simple pendulum, Part II: Longitudinal tuned absorber $G\ddot{\varphi}$ and negative $G\varphi^n$ feedback", Mathematical and Computational Applications 11(2) (2006) 151-162.
21. Amer YA., "Vibration control of ultrasonic cutting via dynamic absorber", Chaos, Solutions & Fractals 33 (2007) 1703-1710.
22. Nayfeh AH., "Introduction to Perturbation Techniques", John Wiley & Sons, Inc., New York, (1981).

23 Hamed, Y.S., EL-Ganaini, W., Kamel M. M.: Vibration suppression in ultrasonic machining described by non-linear differential equations, Journal of Mechanical Science and Technology 23(8) (2009) 2038-2050.
24 Hamed, Y.S., EL-Ganaini, W., Kamel M. M.: Vibration suppression in multi-tool ultrasonic machining to multi-external and parametric excitations, Acta Mechanica Sinica 25 (2009) 403–415.
25 Hamed, Y.S., EL-Ganaini, W., Kamel M. M.: Vibration reduction in ultrasonic machine to external and tuned excitation forces, Applied Mathematical Modeling. 33 (2009) 2853-2863.

Received: October, 2010